Platelet Factor-4 Variant Chemokine CXCL4L1 Inhibits Melanoma and Lung Carcinoma Growth and Metastasis by Preventing Angiogenesis

Sofie Struyf,[1] Marie D. Burdick,[2] Elke Peeters,[1] Karolien Van den Broeck,[1] Chris Dillen,[1] Paul Proost,[1] Jo Van Damme,[1] and Robert M. Strieter[2]

[1]Laboratory of Molecular Immunology, Rega Institute, Leuven, Belgium and [2]Department of Medicine, University of Virginia, Charlottesville, Virginia

Abstract

The platelet factor-4 variant, designated PF-4var/CXCL4L1, is a recently described natural non-allelic gene variant of the CXC chemokine platelet factor-4/CXCL4. PF-4var/CXCL4L1 was cloned, and the purified recombinant protein strongly inhibited angiogenesis. Recombinant PF-4var/CXCL4L1 was angiostatically more active (at nanomolar concentration) than PF-4/CXCL4 in various test systems, including wound-healing and migration assays for microvascular endothelial cells and the rat cornea micropocket assay for angiogenesis. Furthermore, PF-4var/CXCL4L1 more efficiently inhibited tumor growth in animal models of melanoma and lung carcinoma than PF-4/CXCL4 at an equimolar concentration. For B16 melanoma in nude mice, a significant reduction in tumor size and the number of small i.t. blood vessels was obtained with i.t. applied PF-4var/CXCL4L1. For A549 adenocarcinoma in severe combined immunodeficient mice, i.t. PF-4var/CXCL4L1 reduced tumor growth and microvasculature more efficiently than PF-4/CXCL4 and prevented metastasis to various organs better than the angiostatic IFN-inducible protein 10/CXCL10. Finally, in the syngeneic model of Lewis lung carcinoma, PF-4var/CXCL4L1 inhibited tumor growth equally well as monokine induced by IFN-γ (Mig)/CXCL9, also known to attract effector T lymphocytes. Taken together, PF-4var/CXCL4L1 is a highly potent antitumoral chemokine preventing development and metastasis of various tumors by inhibition of angiogenesis. These data confirm the clinical potential of locally released chemokines in cancer therapy. [Cancer Res 2007;67(12):5940–8]

Introduction

Platelet factor-4 (PF-4) has been biochemically characterized as a platelet product with high affinity for heparin long before the term chemokine was introduced to designate small inducible chemotactic cytokines binding to G protein–coupled receptors (GPCR) and attracting various leukocyte subsets to inflammatory sites (1, 2). The position of the conserved cysteines has been used to classify PF4/CXCL4 among the CXC chemokines along with the later discovered granulocyte chemoattractant interleukin-8 (IL-8)/CXCL8 (3). Subsequently, two functional receptors were identified for IL-8/CXCL8 [i.e., CXC chemokine receptor 1 and 2 (CXCR1 and CXCR2)]. Furthermore, IL-8/CXCL8 and other neutrophil-attracting CXC chemokines binding to CXCR2 were shown to possess angiogenic activity (4–6). In contrast to IL-8/CXCL8, the CXCR3 ligands, monokine induced by IFN-γ (Mig)/CXCL9, IFN-inducible protein 10 (IP-10)/CXCL10, and IFN-inducible T-cell α chemoattractant (I-TAC)/CXCL11 are angiostatic and predominantly attract T lymphocytes and natural killer (NK) cells (7–10). The fact that the existence of a functional GPCR for PF-4/CXCL4 has been difficult to elucidate allows us to speculate that its pleiotropic biological activities, such as promotion of neutrophil and monocyte cell adhesion to endothelium and inhibition of angiogenesis, are mediated through different cellular mechanisms, including glycosaminoglycan in addition to GPCR binding (11–15). Indeed, PF-4/CXCL4 has significant antitumoral activity by inhibition of GPCR-mediated endothelial cell chemotaxis, whereas its procoagulant activity is mediated by heparin binding (16–19). Its role in thrombosis and in megakaryopoiesis was confirmed by generation of PF-4/CXCL4 knockout mice (20). However, for several biological effects ascribed to PF-4/CXCL4 (e.g., in atherosclerosis and hematopoiesis; refs. 21, 22), the precise underlying molecular mechanisms are complex and remain partially elusive.

In a previous study, we isolated and identified the PF-4 variant CXCL4L1 from thrombin-stimulated platelets (23). It was shown that natural PF-4var/CXCL4L1 is a more potent inhibitor of endothelial cell chemotaxis and angiogenesis than the well-characterized PF-4/CXCL4, whereas other biological characteristics of PF-4var/CXCL4L1 remain unknown. Here, we confirm *in vitro* activities with recombinant PF-4var/CXCL4L1 at nanomolar concentrations and show that this angiostatic chemokine is a stronger inhibitor of tumor growth and metastasis than PF-4/CXCL4 using different tumor models. PF4var/CXCL4L1 was more potent than IP-10/CXCL10 in preventing tumor metastasis in immunocompromised animals, whereas it had equal antitumoral activity as Mig/CXCL9 in immunocompetent mice. Finally, we provide evidence that antitumoral effects of PF-4var/CXCL4L1 observed at low chemokine dose are predominantly mediated by inhibition of angiogenesis.

Materials and Methods

Reagents and tumor cell lines. Natural human PF-4/CXCL4 and human PF-4var/CXCL4L1 were purified to homogeneity as described (23). Recombinant human basic fibroblast growth factor (bFGF), human IL-8/CXCL8, murine IP-10/CXCL10, and murine Mig/CXCL9 were purchased from R&D Systems.

B16 melanoma was orthotopically propagated in C57Bl/6 mice and cultured in Eagle's minimal essential medium with Earle's salts buffered

Note: Supplementary data for this article are available at Cancer Research Online (http://cancerres.aacrjournals.org/).

S. Struyf is a senior research assistant of the FWO-Vlaanderen.

Requests for reprints: Jo Van Damme, Laboratory of Molecular Immunology, Rega Institute, K.U. Leuven, Minderbroedersstraat 10, B-3000 Leuven, Belgium. Phone: 3216337348; Fax: 3216337340; E-mail: jo.vandamme@rega.kuleuven.be.

doi:10.1158/0008-5472.CAN-06-4682

with $NaHCO_3$ and supplemented with 10% fetal bovine serum (FBS) and L-glutamine. The A549 adenocarcinoma and weakly immunogenic Lewis lung carcinoma (LLC) cell lines were obtained from the American Type Culture Collection and cultured as described (24, 25).

Cloning and purification of recombinant PF-4var/CXCL4L1. The coding region of human PF-4var/CXCL4L1 cDNA was cloned from a human platelet cDNA preparation in two consecutive steps. First, a rather long PF-4var/CXCL4L1 cDNA fragment was amplified by primers specifically binding PF-4var/CXCL4L1 and not PF-4/CXCL4 (5′-TATA*GAATTC*CAGGGAGTCACTGCCTGCAGAACC-3′ as forward primer and 5′-TATA*CTCGAG*GATTGAAAGTGCACACTTAGGCAGC -3′ as backward primer; respective *Eco*RI and *Xho*I sites are in italic). The amplicon (445 bp) was cloned into the pBluescript II vector (Stratagene). The reconstructed phagemid was verified by both restriction analysis and DNA sequencing. This construct was used as a template to amplify the coding region of the mature PF-4var/CXCL4L1 protein (5′-TATA*CCATGG*CCGAAGCTGAAGAAAGATGGGGACCTG-3′ as forward primer and 5′-TATA*CTCGAG*GCTAGGTAGCTAACTCTCCAAATGTTCC-3′ as backward primer; respective *Nco*I and *Xho*I sites are in italic). The PCR reaction product was gel-purified, restriction-digested with *Nco*I and *Xho*I, and ligated into the corresponding sites of the pHEN1 expression vector (26), which contained a LacZ promoter and a PelB leader sequence to direct the expression product to the bacterial periplasm. Verification of the sequence of pHEN1 PF-4var/CXCL4L1 was done on both strands. The ligation mixture was transformed into *Escherichia coli* XL1-Blue cells (Stratagene). For recombinant protein production, the transformed cells were grown in SOC medium containing ampicillin (100 μg/mL) and supplemented with 0.1% glucose at 37°C with shaking to the mid-logarithmic phase (A_{585}, 0.55). At this cell density, isopropyl-L-thio-B-D-galactopyranoside (final concentration, 0.5 mmol/L) was added for induction of PF-4var/CXCL4L1 expression, and incubation was continued for another 4 h followed by harvesting of the cells and preparation of the periplasmic fraction, as described (26). The harvested periplasm was stabilized by addition of a bacterial protease inhibitor cocktail and kept frozen at −20°C until purification.

Pure recombinant PF-4var/CXCL4L1 was obtained from the periplasmic fraction by a purification procedure previously described (23, 27). In a first step, crude periplasmic recombinant PF-4var/CXCL4L1 was purified by heparin-Sepharose affinity chromatography and analyzed by SDS-PAGE and silver staining. Subsequently, fractions enriched in PF-4/CXCL4 immunoreactivity were purified to homogeneity by reversed-phase high-performance liquid chromatography (RP-HPLC). After adjustment of the pH [from pH 7.4 to pH 2.0 with 1% trifluoroacetic acid (TFA) in H_2O], pooled heparin-Sepharose fractions containing PF-4var/CXCL4L1 were injected on a RP-HPLC column equilibrated with 0.1% TFA in H_2O (Source 5 RPC column, Amersham Biosciences/GE Healthcare Bio-Sciences Corp.) and eluted in an acetonitrile (0–80%) gradient (1-mL fractions). Proteins eluting from the RP-HPLC column were analyzed by mass spectrometry on an electrospray ion trap mass spectrometer (Esquire, Bruker) and analyzed for endotoxin contamination by the *Limulus* amebocyte lysate test (Cambrex Bio Science).

Endothelial cell migration. Inhibition of endothelial cell migration *in vitro* was assayed in two different experimental settings. For the *in vitro* wound-healing assay, human dermal microvascular endothelial cells (HMVEC-d; Cambrex Bio Science) were cultured in 24-well plates in EBM-2 medium with the EGM-2-MV Bulletkit (Cambrex Bio Science). When HMVEC were grown to confluency, the culture medium was replaced with 0.5 mL per well EBM-2 medium with 40 μg/mL mitomycin C, without EGM-2-MV Bulletkit. After 30 min at 37°C and 5% CO_2, a plastic pipette tip was used to draw a linear "wound" in the cell monolayer of each well. The monolayers were washed twice with PBS to remove the cells that were detached from the monolayer, and chemokines were added in EBM-2 medium with EGM-2-MV Bulletkit (0.5 mL per well). After 36 to 48 h, HMVEC cultures were fixed and stained with Hemacolor staining solutions. In every 24-well plate, three control cultures were included to which no chemokine was added. The difference of the width before and after treatment of the individual wounds were scored under a microscope and set at zero for control cultures. A wound that was broader compared with control scars (inhibition of HMVEC migration) received an inhibition score and ranged from −3 (very broad) to 0. All samples were tested in triplicate in each 24-well plate and were scored double blind by three investigators. Digital pictures from representative wells were taken with a Canon G3 camera mounted on a Carl Zeiss Axiovert 40 CFL microscope with an A-plan ×10/0.25 objective (Carl Zeiss).

The Boyden chamber assay for endothelial cells has been described previously (28). For this assay, human lung microvascular endothelial cells (HMVEC-L; Cambrex Bio Science) were cultured following the manufacturer's instructions.

Cornea assay. Analysis of the *in vivo* angiostatic activity of recombinant PF-4var/CXCL4L1 was done in hooded Long-Evans rat eyes as described previously (5, 23).

Tumor models. Animal experiments were approved by the local animal ethics committees [University of Leuven and University of California, Los Angeles (UCLA)] and conducted in conformity with the Belgian, European and U.S. guidelines for the protection of animals used for scientific purposes. B16 experiments were done with 6- to 8-week-old female athymic *nu/nu* mice (NMRI background) kept in a specific pathogen-free environment (Elevage Janvier). B16 melanoma cells in log phase (2×10^6 cells resuspended in 200 μL of PBS) were injected s.c. on day 0 in the right dorsal flank. Animals were injected at the tumor site with 50 μL of test sample [i.e., endotoxin-free saline (0.9% NaCl, Baxter), 5 μg of natural human PF-4/CXCL4, or 1 μg of recombinant human PF-4var/CXCL4L1 in saline]. All animals were observed thrice a week, and the tumor dimensions were measured with calipers. For immunohistochemical analysis of tumor vasculature, tumors were harvested and snap frozen in liquid N_2, and sections were analyzed for the presence of blood vessels reacting with rat anti-mouse CD31 antibody (PharMingen/BD Biosciences) using the anti-rat immunoglobulin horseradish peroxidase detection kit from PharMingen and were microscopically evaluated on a Carl Zeiss Axiovert-200M. Digital pictures from representative slides were taken with a MRc5 camera (Carl Zeiss) and a Plan Apochromat ×20/0.8 objective.

CB-17 severe combined immunodeficient (SCID) mice (6–8 weeks old; UCLA Animal Core Facility, Los Angeles, CA) and C57Bl/6 mice (Jackson Labs) were injected s.c. into the right flank with 10^6 A549 cells or 10^6 LLC cells in 100 μL, respectively. Mice were treated with i.t. injections of 20 μL of chemokine solution (or PBS supplemented with 1 mg/mL human serum albumin as vehicle control) thrice a week. Once palpable tumors were visible, tumors were measured in two dimensions with calipers on a weekly basis. At 4 weeks (LLC) or 8 weeks (A549) after tumor cell injection, animals were euthanized by pentobarbital overdose, and the tumors were resected, removed of extraneous tissue, and measured. A portion of the resected tumors was fixed in 4% formaldehyde for histologic analysis. Another portion of the tumors was used for flow cytometry (29). Briefly, two 6-mm tumor punches (determination of angiogenesis) or whole organs (determination of leukocyte influx or metastasis) were minced and digested in 5 mL of 1 mg/mL type IV collagenase (Roche Applied Sciences) for 45 min at 37°C with constant agitation in a water bath. Single-cell suspensions were obtained by repeatedly aspirating the cell suspensions through the bore of a 18-mL syringe. RBC lysis was done for 3 min at room temperature in lysis buffer [0.15 mol/L NH_4Cl, 0.1 mmol/L $KHCO_3$, 0.1 mmol/L Na_2EDTA (pH 7.2)]. Intermediate wash steps were done using fluorescence-activated cell sorting (FACS) buffer (1% FBS and 0.1% sodium azide in PBS). Finally, cell suspensions were passed over a 70-μm nylon mesh; the total cell count was determined; and cells were resuspended in FACS buffer to 1×10^7 cells per milliliter. Samples (100 μL) were stained at 4°C for the presence of endothelial cells using the panendothelial cell marker MECA-32 (BD Biosciences) and analyzed by FACS. First, the percentage of endothelial cell marker–positive cells was determined. Subsequently, the total number of endothelial cells inside a tumor was obtained by multiplication with the determined tumor volume. Single-cell suspensions were also prepared to quantify leukocyte influx in tumors. Total leukocyte, monocyte, and neutrophil counts were determined by FACS analysis using anti-CD45 (BD Biosciences), Moma-2 (AbD Serotec), and anti-Gr-1

antibodies (BD Biosciences), respectively. For detection of metastasis of human A549 cells, phycoerythrin-conjugated anti-human CD49b (BD Biosciences) was used. From the percentage of $CD49b^+$ cells, the total number of human cells per organ was calculated. For determination of the number of metastatic cells in the circulation, the results are expressed per milliliter of blood.

Statistical analysis. All data were analyzed using the Statview 4.5 statistical software package (Abacus Concepts, Inc.) or Statistica (StatSoft, Inc.). All animal group comparisons were evaluated by the ANOVA test with Bonferroni/Dunn post hoc analysis, unless otherwise indicated in the figure legend. Data are expressed as mean ± SEM.

Results

Functional characterization of recombinant PF-4var/CXCL4L1 *in vitro* and *in vivo*. PF-4var/CXCL4L1 expressed in *E. coli* was purified to homogeneity by heparin-Sepharose affinity chromatography and subsequent RP-HPLC (data shown in Supplementary Data). Pure recombinant 8-kDa CXCL4L1 protein eluted from both types of columns at a similar position as natural PF-4var/CXCL4L1 and corresponded to the major peak of PF-4 immunoreactivity determined by ELISA. Recombinant PF-4var/CXCL4L1 was confirmed to have the correct molecular mass upon SDS-PAGE and mass spectrometry analysis. Furthermore, the NH_2-terminal sequence was verified by Edman degradation on an automated protein sequencer (data not shown). The biological activity of recombinant PF-4var/CXCL4L1 was evidenced in the *in vitro* wound-healing assay on mitomycin C–treated human microvascular endothelial cells (Fig. 1*A* and *B*). Figure 1*B* shows that recombinant PF-4var/CXCL4L1 significantly inhibited endothelial cell migration at 10 ng/mL, whereas natural PF-4/CXCL4 only did so at 200 and 1,000 ng/mL. Furthermore, in the endothelial cell migration assay using the Boyden chamber, recombinant PF-4var/CXCL4L1 very efficiently inhibited the chemotactic activity of both IL-8/CXCL8 and bFGF from 5 ng/mL onwards, whereas natural PF-4/CXCL4 only marginally affected endothelial cell chemotaxis at 50 ng/mL (Fig. 1*C*). This stronger *in vitro* potency of recombinant PF-4var/CXCL4L1 to inhibit endothelial cell migration was finally confirmed in the rat cornea micropocket assay for angiogenesis (n = 6 for each treatment). In this *in vivo* test, angiogenic IL-8/CXCL8 (80 ng per pellet) or bFGF (50 ng per

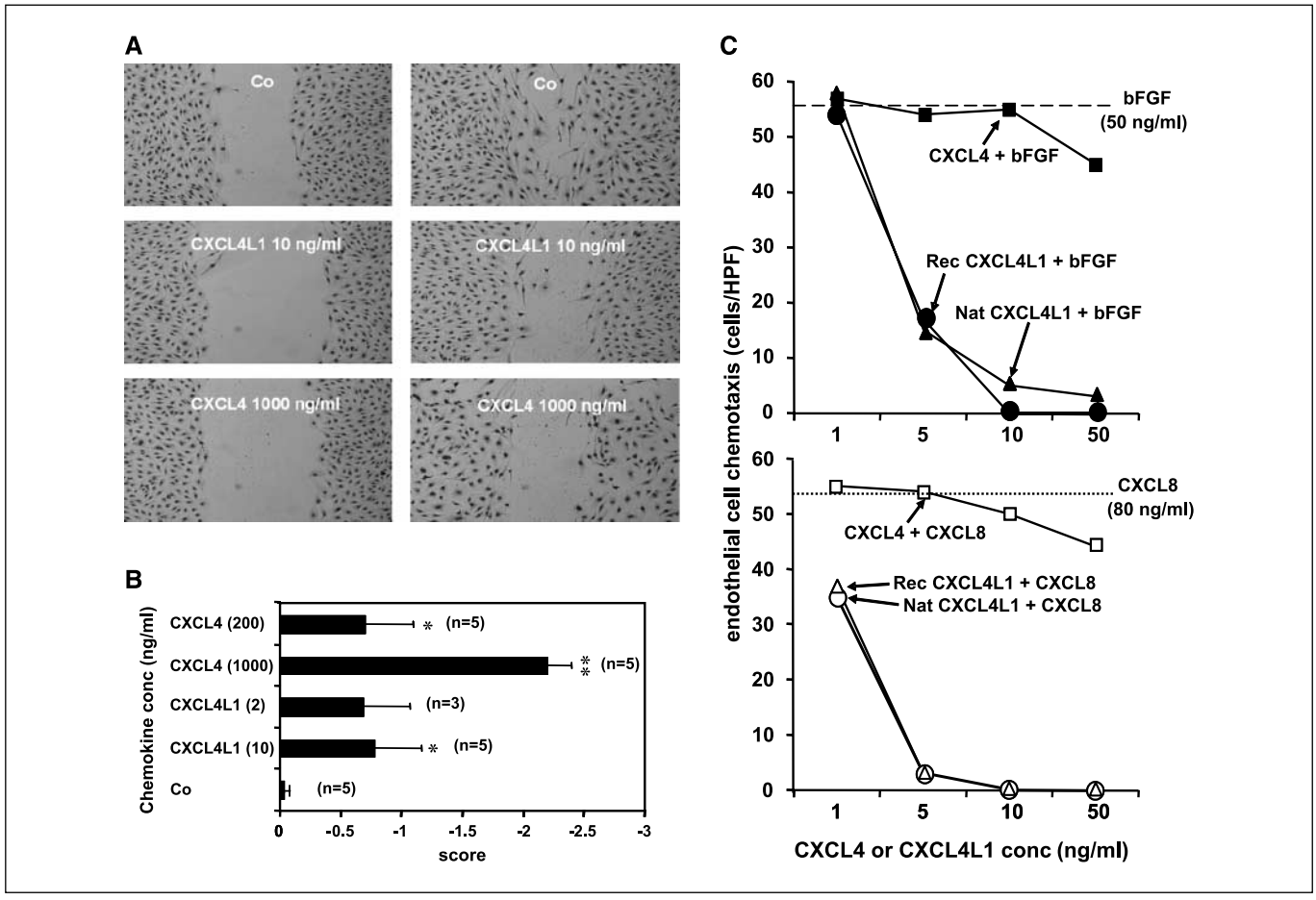

Figure 1. *In vitro* characterization of recombinant PF-4var/CXCL4L1. Recombinant PF-4var/CXCL4L1 was tested in the *in vitro* wound-healing assay for inhibition of endothelial cell migration (*A* and *B*). Confluent monolayers of HMVEC-d were scarred, and repair was monitored microscopically after 42-h treatment with recombinant CXCL4L1 (2 or 10 ng/mL) or CXCL4 (200 or 1,000 ng/mL). Zero scores correspond to the change in wound width for untreated control cultures (*Co*). A wound that retained a broader width compared with control wounds (inhibition of migration) received a negative score. *A,* representative photographs taken from two different experiments. *B, columns,* average changes in scores from three to five independent experiments; *bars,* SEM. *, $P < 0.05$; **, $P < 0.01$, statistically significant inhibition (Mann-Whitney test). In the Boyden chamber assay (*C*), recombinant (*rec*) CXCL4L1 (1–50 ng/mL) was compared with natural (*nat*) CXCL4L1 (1–50 ng/mL) and CXCL4 (1–50 ng/mL) for its capacity to reduce migration of HMVEC-L toward bFGF (50 ng/mL) or CXCL8 (80 ng/mL). To show specific migration, background (unstimulated control) migration (45 cells per high-power field) was subtracted. Results are derived from two independent experiments in triplicate. Angiogenic activity of bFGF (*broken lines*) and CXCL8 (*dotted lines*).

pellet) were 70% to 80% inhibited by both natural and recombinant PF-4var/CXCL4L1 at 50 ng per pellet, whereas natural PF-4/CXCL4 (50 ng per pellet) had no inhibitory effect on bFGF-induced angiogenesis (data not shown). Applied as single stimulus, IL-8/CXCL8 and bFGF triggered neovascularization in five or six of six corneas, respectively. Taken together, it can be concluded that recombinant PF-4var/CXCL4L1, tested in three different assays, is an at least 10-fold more potent inhibitor of angiogenesis than PF-4/CXCL4. Based on these findings, we aimed to verify whether PF-4var/CXCL4L1 could also exert a more pronounced antitumoral activity.

Comparison of PF-4/CXCL4, PF-4var/CXCL4L1, and angiostatic CXCR3 ligands for the inhibition of melanoma and lung carcinoma growth and metastasis. To assess the antitumoral activity of PF-4var/CXCL4L1, different experimental settings were used. To exclude that leukocyte influx is necessary for the possible antitumoral effect, nude mice lacking functional T cells and SCID beige mice, which lack T and B cells and which also have NK cell dysfunction, were used first, allowing also to evaluate human tumor cells (A549 adenocarcinoma). In addition, PF-4var/CXCL4L1 was analyzed in parallel with chemokines known to attract effector T lymphocytes in an immunocompetent mouse system with syngeneic tumors (LLC in C56Bl/6 mice). With regard to the injected chemokine dose, two different approaches were applied. In the first animal model (B16 melanoma), the antitumoral potency of PF-4var/CXCL4L1 was evaluated in direct comparison with PF-4/CXCL4, for which high doses (50 μg per injection) have previously been applied to obtain antitumoral effects (17, 30). Second, in more prolonged tumor models (lung carcinoma), PF4var/CXCL4L1 was injected at lower doses in comparison with CXCR3 ligands, to which angiostatic activity has been ascribed at much lower doses (0.1 μg per injection; refs. 31, 32).

In a first experimental setting, three groups of 12 to 14 athymic nude mice were each injected s.c. with 2×10^6 B16 melanoma cells and were then i.t. treated (thrice per week; six or seven injections in total) with 5 μg natural PF-4/CXCL4, 1 μg recombinant PF-4var/CXCL4L1, or physiologic saline. Tumor growth, determined by external measurement (thrice per week) of the tumor size, was found to be reduced in the PF-4/CXCL4 and PF-4var/CXCL4L1 groups compared with control mice over the whole period of 17 days, when mice were killed (Fig. 2*A*). Figure 2*B* shows that the resected tumor volume was also significantly reduced ($P = 0.035$) in the PF-4var/CXCL4L1 group (median, 556 mm^3) versus saline-treated mice (median, 940 mm^3), whereas the effect of PF-4/CXCL4 (median, 803 mm^3) was yet not significant at a 5-fold higher dose, indicating a stronger antitumoral potency of the variant PF-4 form. It was next verified whether this antitumoral activity could be mediated by inhibition of angiogenesis. This was evidenced by immunohistochemical evaluation of the i.t. microvasculature using anti-CD31 staining (Fig. 2*C* and *D*). Indeed, the number of small i.t. blood vessels was significantly lower in PF-4var/CXCL4L1-treated mice compared with the PF-4/CXCL4 or saline control group ($P = 0.01$ and 0.02, respectively). The fact that we did not observe a significant antitumoral effect for PF-4/CXCL4 in this tumor model could be due to the lower dose of PF-4/CXCL4 applied compared with previous studies (daily injections of 50 μg) with this angiostatic chemokine (17, 30).

Second, in a model of non–small-cell lung cancer, SCID mice were injected s.c. with 10^6 A549 adenocarcinoma cells and treated i.t. (0.1 μg; thrice a week), with either PF-4/CXCL4, PF-4var/CXCL4L1, or vehicle control. After 4 weeks, tumors were clearly larger in control mice, and in particular, for the PF-4var/CXCL4L1 group, reduced tumor growth was most pronounced after 8 weeks, when mice were sacrificed (Fig. 3*A*). The resected PF-4var/CXCL4L1–treated tumors were on average less than half the size of the control tumors, whereas the PF-4/CXCL4 treatment did not provide a statistically significant decrease in tumor size (Fig. 3*B*). Nevertheless, determination of the angiostatic effect of PF-4 treatment by flow cytometric analysis of single-cell tumoral suspensions revealed significant decreases in MECA-32^+ endothelial cells and confirmed reduced angiogenesis in both the PF-4/CXCL4 ($P = 0.045$) and PF-4var/CXCL4L1 ($P = 0.026$) groups versus control mice (Fig. 3*C*).

We next compared PF-4var/CXCL4L1 with the angiostatic CXCR3 ligand IP-10/CXCL10 upon i.t. injection (0.1 μg; thrice per week) to inhibit growth of human A549 adenocarcinoma in SCID mice. After 8 weeks, tumors in control mice reached volumes (>2,000 mm^3), which were significantly ($P < 0.05$) larger than those ($\pm$1,000 mm^3) in mice treated with PF-4var/CXCL4L1 or IP-10/CXCL10 (Fig. 4*A*). The resected tumor volume was also significantly smaller ($P < 0.017$) for the PF-4var/CXCL4L1 and IP-10/CXCL10 groups versus control mice (Fig. 4*B*), the effect of PF-4var/CXCL4L1 being more pronounced. Moreover, flow cytometric analysis of tumor cell suspensions confirmed the angiostatic potential of the two chemokines, as evidenced by the significantly ($P < 0.01$) reduced number of MECA-32^+ endothelial cells in tumors treated with PF-4var/CXCL4L1 or IP-10/CXCL10 (Fig. 4*C*). This angiostatic effect was confirmed by the detection of increased tumor cell necrosis in chemokine-treated animals (data not shown). Finally, it was observed that metastasis of A549 adenocarcinoma cells to brain, adrenal gland, lung, liver, and blood was significantly ($P < 0.017$) prevented by i.t. PF4var/CXCL4, whereas IP-10/CXCL10 inhibited the number of metastatic cells in the brain only (Table 1). Thus, the antitumoral activity of human PF-4var/CXCL4L1 was found to be more pronounced than that of IP-10/CXCL10 and PF-4/CXCL4 in this SCID/A549 chimeric model of non–small-cell lung cancer. To know whether the antitumoral effect of CXCL4L1/PF-4var is solely based on its angiostatic activity, the influx of leukocytes was excluded. Because SCID mice are devoid of T-cell, B-cell, and NK cell activity, monocyte and neutrophil infiltration was evaluated in this model. FACS analysis of single-cell suspensions prepared from resected tumors of PF-4var/CXCL4L1–treated mice revealed no significant changes in $CD45^+$ leukocytes, whereas in IP-10/CXCL10–treated animals, the number of total leukocytes per tumor volume was doubled (Fig. 4*D*). Because no clearly enhanced influx of Moma-2^+ monocytes and Gr-1^+ granulocytes was observed in PF-4var/CXCL4L1–injected tumors, it can be concluded that leukocyte infiltration (granulocytes, monocytes, T cells, B cells, and NK cells) is not a major determinant in the antitumoral effect of this angiostatic chemokine.

In a third syngeneic model (i.e., LLC in C57Bl/6 mice), the antitumoral potential of PF-4var/CXCL4L1 was compared with that of the angiostatic chemokine Mig/CXCL9 in immunocompetent mice. Figure 5*A* shows that both CXC chemokines (at an i.t. dose of 0.1 μg; thrice per week) gradually inhibited tumor growth over time compared with control mice. A significant reduction ($P < 0.02$) in tumor size was reached 4 weeks after injection of tumor cells. This antitumoral effect was confirmed on resected tumors (Fig. 5*B*) from mice treated with PF-4var/CXCL4L1 ($P = 0.022$) or Mig/CXCL9 ($P = 0.018$). Tumor growth retardation was again due to

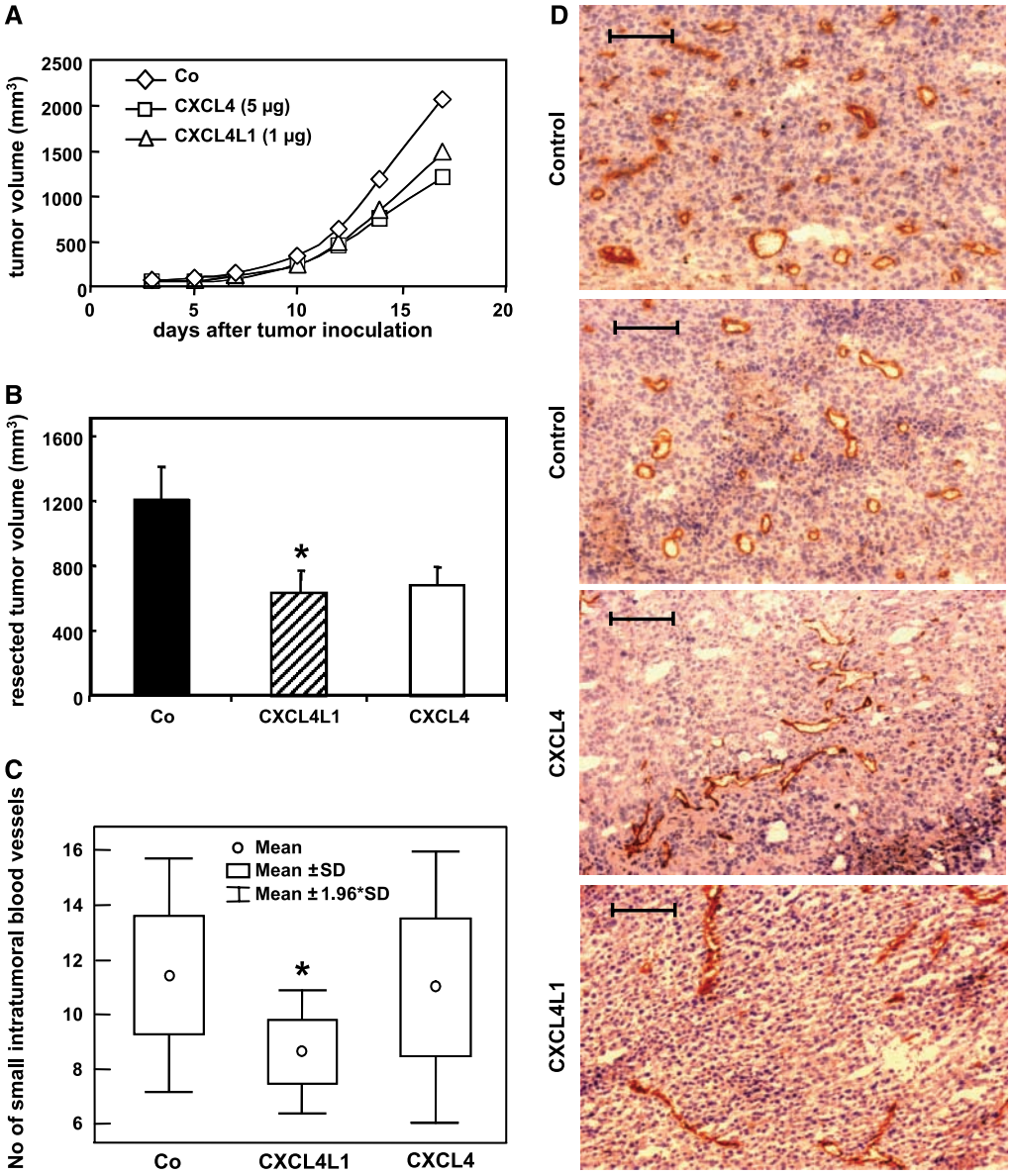

Figure 2. Inhibition of tumor growth and angiogenesis by treatment of B16-melanoma with the angiostatic chemokines PF-4/CXCL4 or PF-4var/CXCL4L1. Mice (*nu/nu* NMRI background, $n = 38$, compilation of two independent experiments) were injected on day 0 with 2×10^6 B16 melanoma cells and divided into three groups, which received 9 g/L NaCl saline ($n = 14$), 5 μg CXCL4 ($n = 12$), or 1 μg CXCL4L1 ($n = 12$) per injection, respectively. Treatment started on day 1 (experiment 2) or day 3 (experiment 1), and saline or chemokines were injected i.t. thrice a week. In total, six (experiment 1) or seven (experiment 2) injections were administered. Tumor dimensions were measured on every day of chemokine injection. Mean values per group were calculated (*A*). At these time points, the tumor volume was calculated using the formula: $(4\pi ab^2) / 3$ (*a* and *b*, largest and smallest radius, respectively). On day 17, tumors were resected, and the dimensions were measured to determine the tumor volume more exactly (*B*), which was calculated by the formula: $(4\pi abc) / 3$ (*a, b*, or *c*, measured radii). *Points/columns,* mean tumor sizes (mm^3) per treatment group; *bars,* SEM. On day 17, resected tumors from the CXCL4L1-treated group were significantly smaller (*, $P = 0.035$) than those from the vehicle-treated group (Mann-Whitney test). The microvasculature in B16 tumors in the 20 mice of experiment 1 treated with 0.9% NaCl saline ($n = 8$), 5 μg CXCL4 ($n = 6$), or 1 μg CXCL4L1 ($n = 6$) per injection was evaluated. Per tumor, four biopsies were frozen and evaluated by immunohistochemistry. Blood vessels were visualized in frozen tissue sections by staining with anti-CD31 (red reaction product localizes to endothelial cells lining blood vessels) followed by a faint counterstain with Mayer's hematoxylin. Per tumor biopsy, 6 high-power fields were evaluated in one representative section by counting the number of vessels present, making a distinction between large and small vessels. Per representative section, the mean number of small and large blood vessels was calculated per high-power field. *C,* box-whisker plot of statistical analysis of the differences in the number of small blood vessels in the three groups of tumor treatment. *D,* representative photographs taken. *Bar*, ~100 μm. The Kruskal-Wallis test (*C*) indicated that the three groups are statistically different ($P = 0.017$). The number of small blood vessels in the group treated with CXCL4L1 was significantly lower than in the groups treated with saline or CXCL4 (Mann-Whitney test, $P = 0.01$ and $P = 0.02$, respectively). Treatment with 5 μg CXCL4 did not significantly influence the number of small blood vessels, when compared with the saline control group. There was no significant difference in the number of large blood vessels per high-power field among the three groups (data not shown, Kruskal-Wallis test).

inhibition of angiogenesis (Fig. 5*C*) as evidenced by the significantly reduced numbers of MECA-32$^+$ endothelial cells by treatment with PF-4var/CXCL4L1 ($P = 0.016$) or Mig/CXCL9 ($P = 0.021$). Taken together, these data show that in three different tumor models using immunocompromised or immunocompetent mice, a clear cut angiostatic effect for PF-4var/CXCL4L1 was noticed, resulting in significant inhibition of tumor growth and metastasis.

Discussion

Chemokines can indirectly stimulate or inhibit tumor growth by their angiogenic or angiostatic activity, respectively (33). Alternatively, chemokines also affect tumor development by attracting immunocompetent cells with protumoral or antitumoral activities. Indeed, tumor-infiltrating leukocytes, such as macrophages, might promote tumor growth and progression (34, 35). However, effector T lymphocytes and NK cells are considered to exert antitumor activity. In this context, CXCR3 ligands, attracting T lymphocytes and NK cells, can inhibit tumor growth. Moreover, these chemokines are also antitumoral by inhibiting endothelial cell proliferation and migration through GAG and/or CXCR3 binding (13, 33). In contrast, tumor growth inhibition by PF-4/CXCL4 is expected to occur predominantly via its angiostatic activity, rather than by attracting effector lymphocytes. In this study, the recently identified PF-4var/CXCL4L1 (23) was compared with authentic PF-4/CXCL4 and the CXCR3 ligands Mig/CXCL9 and IP-10/CXCL10 and was found to inhibit tumor growth and angiogenesis more efficiently in different animal models.

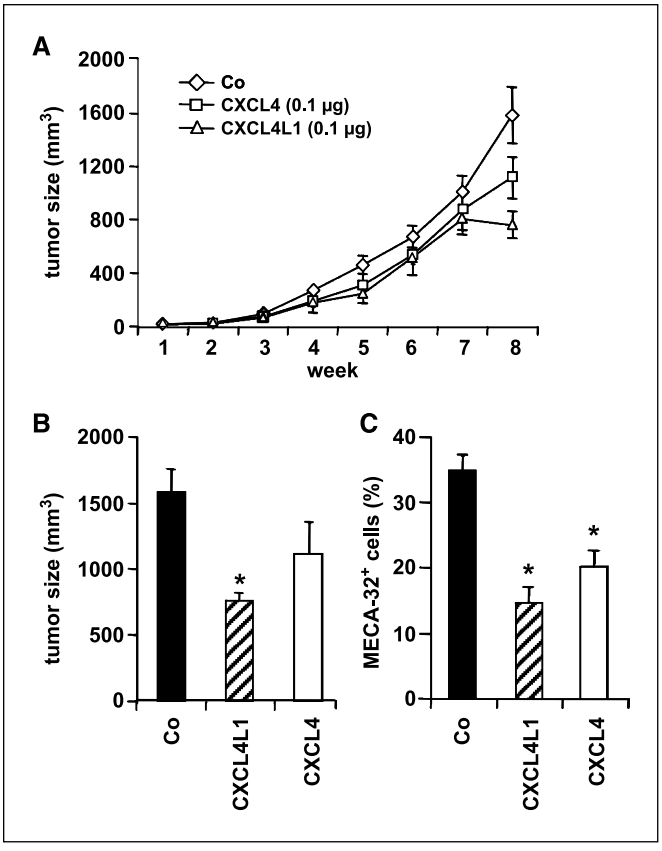

Figure 3. Inhibition of tumor growth and angiogenesis by treatment of A549 adenocarcinoma with PF-4var/CXCL4L1 in comparison with PF-4/CXCL4. CB-17 SCID mice were injected s.c. on day 0 with A549 adenocarcinoma cells and divided into three groups, which received vehicle control (n = 10), 0.1 μg CXCL4L1 (n = 10), or 0.1 μg CXCL4 (n = 10) per injection, respectively. Treatment started at the time of tumor inoculation. Chemokines were injected i.t. thrice a week, and tumor dimensions were measured every week (*A*). At these time points, the tumor volume was calculated using the formula: $(4\pi ab^2) / 3$ (*a* and *b*, largest and smallest radius, respectively). After 8 wks, mice were sacrificed, and exact tumor dimensions were determined (*B*), which was calculated by the formula: $(4\pi abc) / 3$ (*a, b*, or *c*, measured radius). *Points/columns,* mean tumor size (mm^3) per treatment group; *bars,* SEM. Per group, six tumors were minced into single-cell suspensions for flow cytometric analysis. In these cell suspensions, % MECA-32$^+$ endothelial cells was determined to monitor angiogenesis in the tumors (*C*). *, $P < 0.05$, statistically significant difference between the control group and the mice treated with CXCL4L1 or CXCL4.

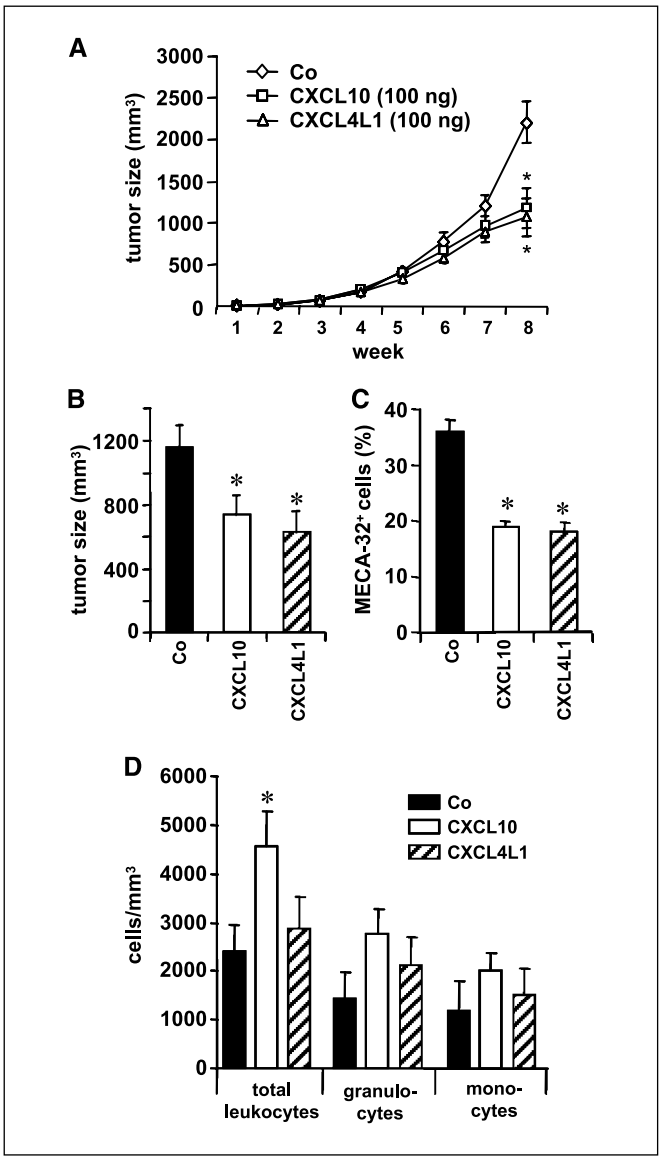

Figure 4. Treatment of A549 adenocarcinoma with the angiostatic chemokines PF-4var/CXCL4L1 or IP-10/CXCL10. Mice (SCID Beige) were injected s.c. on day 0 with A549 adenocarcinoma cells and divided into three groups, which received vehicle control (n = 10), 0.1 μg human CXCL4L1 (n = 10), or 0.1 μg murine CXCL10 (n = 10) per injection, respectively. Treatment started at the time of tumor inoculation. Chemokines were injected i.t. thrice a week, and tumor dimensions were measured every week (*A*). After 8 wks, mice were sacrificed, and exact tumor dimensions were determined (*B*). The formulas used to calculate tumor volumes are mentioned in Fig. 3 legend. *Points/columns,* mean tumor size (mm^3) per treatment group; *bars,* SEM. Per group, five tumors were minced into single-cell suspensions for flow cytometric analysis. In these cell suspensions, % endothelial cells (MECA-32$^+$) was determined to monitor angiogenesis in the tumors (*C*). In addition, the cell suspensions were analyzed for leukocyte content by FACS analysis (*D*). The total number of leukocytes (CD45$^+$ cells), monocytes/macrophages (Moma-2$^+$ cells), and granulocytes (Gr-1$^+$ cells) was determined per tumor volume. *, $P < 0.05$, statistically significant difference between the control group and the mice treated with CXCL4L1 or CXCL10.

First, it was shown that recombinant PF-4var/CXCL4L1 is at least 10-fold more potent than PF-4/CXCL4 in preventing endothelial cell migration, as tested in the *in vitro* wound-healing

Table 1. Impaired metastasis of A549 adenocarcinoma treated with the angiostatic chemokines PF-4var/CXCL4L1 or IP-10/CXCL10

Group	Total no. metastatic cells per organ ± SEM*					
	Brain ($\times 10^6$)	Adrenal gland ($\times 10^4$)	Lung ($\times 10^6$)	Liver ($\times 10^5$)	Blood ($\times 10^3$/mL)	Bone Marrow ($\times 10^4$)
Control	3.1 ± 0.4	1.1 ± 0.2	1.5 ± 0.1	4.1 ± 0.4	2.9 ± 8.8	2.0 ± 0.2
CXCL10	2.1 ± 0.2 †	0.6 ± 0.2	1.2 ± 0.1	3.5 ± 0.5	1.9 ± 2.3	1.9 ± 0.3
CXCL4L1	1.7 ± 0.3 †	0.4 ± 0.1 †	1.0 ± 0.2 †	1.3 ± 0.4 †	1.1 ± 1.8 †	1.7 ± 0.3

*Mice were injected with A549 cells and divided into three groups, which received vehicle control (n = 10), 0.1 μg human CXCL4L1 (n = 10), 0.1 μg murine CXCL10 (n = 10) per injection, respectively, as indicated in Fig. 4 legend. Different organs known to be invaded by A549 lung adenocarcinoma cells were minced into single-cell suspensions for flow cytometric analysis (six mice per group), and the number of human cells was determined.
† $P < 0.0167$, statistically significant difference between the control group and the mice treated with CXCL4L1 or CXCL10.

assay and the Boyden chamber migration assay on human microvascular endothelial cells. This finding was confirmed by the *in vivo* rat cornea micropocket assay for angiogenesis. Second, this stronger potency of PF-4var/CXCL4L1 compared with PF-4/CXCL4 was also shown upon i.t. injection in the rapidly progressing B16 melanoma model (2 weeks) using athymic nude mice in which the effect of infiltrating lymphocytes is excluded. Furthermore, reduction in tumor size by PF-4var/CXCL4L1 was paralleled by a significantly lowered presence of i.t. microvasculature as evidenced by CD31 staining. Similar results were obtained in a slower progressing model of non–small-cell lung carcinoma (8 weeks), in which PF-4var/CXCL4L1 inhibited the growth of human A549 cells in SCID mice more efficiently than PF-4/CXCL4. Angiostasis again accounted for the antitumoral effect of both PF-4 forms as evidenced by flow cytometric analysis of the tumors. I.t. injection of PF4var/CXCL4L1 or IP-10/CXCL10 at equimolar concentrations revealed a comparable reduction in A549 tumor size, paralleled with an equal inhibition of tumoral angiogenesis. However, upon injection of PF-4var/CXCL4L1, the metastatic behavior of the tumor was more impaired compared with IP-10/CXCL10 or buffer treatment. Because SCID beige mice have deficiencies in the lymphocyte lineage functions (lacking T and B cells and having impaired NK cell function), these data show that lymphocyte recruitment is not required for the inhibition of tumor growth and metastasis by PF-4var/CXCL4L1. In addition, analysis of tumor-associated leukocytes in the A549/SCID beige model revealed no statistically significant difference in the number of monocytes and granulocytes in the PF-4var/CXCL4L1–treated tumors compared with buffer treated tumors. Finally, it was found that in the syngeneic model of LLC (4 weeks) PF-4var/CXCL4L1 and the CXCR3 ligand Mig/CXCL9 both significantly inhibited tumor growth, which was paralleled with an equal reduction in i.t. endothelial cells. In this model using immunocompetent mice, the effect of infiltrating tumor-associated leukocytes can not be excluded, especially with regard to the potential attraction of antitumoral Th1 effector cells by Mig/CXCL9.

The molecular basis of the angiostatic and antitumoral activities of the PF-4 forms remains an enigma, although for CXCL4, several mechanisms have been proposed (36). The findings that PF-4var/CXCL4L1 and the CXCR3 ligands IP-10/CXCL10 and Mig/CXCL9 can inhibit the angiogenic effect of IL-8/CXCL8 indicate that GPCR are probably implicated (33). Indeed, CXCR2 is expressed on endothelial cells and could be responsible for the angiogenic activity of IL-8/CXCL8 and other CXC chemokines using this receptor (28). However, it is still unknown how angiostatic CXCR3 ligands can molecularly prevent angiogenesis induced by CXCR2 ligands. Yang and Richmond indicate that for the angiostatic activity of IP-10/CXCL10 in tumors, CXCR3 receptor binding but not glycosaminoglycan binding is essential (37). Alternatively, Soejima and Rollins found a functional receptor for IP-10/CXCL10 on endothelial cells, which is neither CXCR3 nor glycosaminoglycan

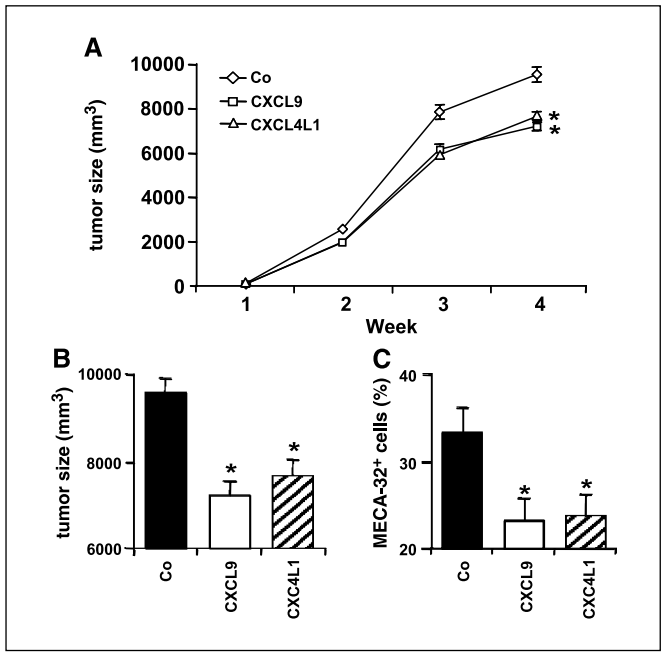

Figure 5. Reduced tumor growth and vascularity after treatment of LLC with the angiostatic chemokines PF-4var/CXCL4L1 or Mig/CXCL9. Mice (C57Bl/6; n = 30) were injected s.c. on day 0 with LLC cells and divided into three groups, which received vehicle control (n = 10), 0.1 μg human CXCL4L1 (n = 10), or 0.1 μg murine CXCL9 (n = 10) per injection, respectively. Treatment started at the time of tumor inoculation. Chemokines were injected i.t. thrice a week, and tumor dimensions were measured every week (*A*). After 4 wks, mice were sacrificed, and exact tumor dimensions were determined (Panel *B*). The formulas used to calculate tumor volumes are mentioned in Fig. 3 legend. *Points/columns,* mean tumor size (mm^3) per treatment group; *bars,* SEM. To assess tumor vascularity, six tumors per group were minced into single-cell suspensions for flow cytometric analysis using the panendothelial cell marker MECA-32 (*C*). *, $P < 0.05$, statistically significant difference between the control group and the mice treated with CXCL4L1 or CXCL9.

(38). The report that human PF-4/CXCL4 is a ligand for a variant of CXCR3 (i.e., CXCR3B; ref. 15) does not clarify the issue because there is no evidence for the existence of CXCR3B in mice, and human PF-4 forms are angiostatic in mice against both human and mouse tumors. Furthermore, the NH_2-terminal part of chemokines has been considered as essential for receptor binding (39). In this context, it is surprising that COOH-terminal fragments of PF-4/CXCL4 are equally or more angiostatic compared with intact chemokine (40). Because the COOH-terminal part of CXCL4 interacts with glycosaminoglycans, it has been suggested that this part is important for the angiostatic activity of PF-4/CXCL4 by preventing the binding of growth factors to their receptor (13, 36). However, PF-4var/CXCL4L1 has less affinity for heparin than PF-4/CXCL4 while being more angiostatic, indicating that a combined effect of binding to both GAG and GPCR might be implicated. Finally, it has been shown that PF-4/CXCL4 can form inactive complexes with IL-8/CXCL8 (41) as well as with bFGF (42). The angiogenic activity of IL-8/CXCL8 and bFGF is strongly inhibited by PF-4var/CXCL4L1 (23), and one could speculate that PF-4var/CXCL4L1 is more efficiently complexed with these angiogenic factors. Definitively, further experimental work is necessary to elucidate the molecular mechanisms through which PF-4 variants inhibit angiogenesis, exploring chemokine, GAG, as well as GPCR binding.

It is generally accepted that chemokines can be detrimental for tumor development and progression, despite the fact that tumor cell–derived chemokines may be beneficial for tumor growth (refs. 34, 35; e.g., by attracting leukocytes loaded with proteases that can promote tumor invasion and metastasis; ref. 43). In addition, the expression of chemokine receptors contributes to metastasis of tumor cells to the organs where the corresponding chemokine is produced (44). Antitumoral activity of locally delivered chemokine has been tested for several CXC and CC chemokines. Application of engineered tumor cells or oncotropic viruses (e.g., parvovirus) to locally release chemokines, such as monocyte chemotactic protein-3 (MCP-3)/CCL7 and Mig/CXCL9 in melanoma and lung carcinoma, confirms their potential clinical value in anticancer therapy (32, 45). Furthermore, such approach can be applied as a combination therapy in which chemokines (e.g., CXCR3 ligands) and cytokines (such as IL-2 and IL-12) are co-delivered to reach both an optimal angiostatic and immunogenic antitumoral effect (46, 47).

Acknowledgments

Received 12/20/2006; revised 3/16/2007; accepted 4/17/2007.

Grant support: Center of Excellence (credit no. EF/05/15) of K.U. Leuven, the Concerted Research Actions of the Regional Government of Flanders, the Fund for Scientific Research of Flanders (FWO-Vlaanderen), the Interuniversity Attraction Poles Program-Belgian Science Policy, the European Union 6FP EC contract INNOCHEM, and NIH grants CA87879, P50CA90388, HL66027, and P50HL67665 (R.M. Strieter).

The costs of publication of this article were defrayed in part by the payment of page charges. This article must therefore be hereby marked *advertisement* in accordance with 18 U.S.C. Section 1734 solely to indicate this fact.

We thank René Conings and Jean-Pierre Lenaerts for their expert technical assistance.

References

1. Deuel TF, Keim PS, Farmer M, Heinrikson RL. Amino acid sequence of human platelet factor 4. Proc Natl Acad Sci U S A 1977;74:2256–8.
2. Brandt E, Ludwig A, Petersen F, Flad HD. Platelet-derived CXC chemokines: old players in new games. Immunol Rev 2000;177:204–16.
3. Van Damme J, Van Beeumen J, Opdenakker G, Billiau A. A novel, NH_2-terminal sequence-characterized human monokine possessing neutrophil chemotactic, skin-reactive, and granulocytosis-promoting activity. J Exp Med 1988;167:1364–76.
4. Murphy PM, Tiffany HL. Cloning of complementary DNA encoding a functional human interleukin-8 receptor. Science 1991;253:1280–3.
5. Strieter RM, Polverini PJ, Kunkel SL, et al. The functional role of the ELR motif in CXC chemokine-mediated angiogenesis. J Biol Chem 1995;270:27348–57.
6. Rot A, Von Andrian UH. Chemokines in innate and adaptive host defense: basic chemokinese grammar for immune cells. Annu Rev Immunol 2004;22:891–928.
7. Luster AD, Unkeless JC, Ravetch JV. Gamma-interferon transcriptionally regulates an early-response gene containing homology to platelet proteins. Nature 1985;315:672–6.
8. Farber JM. HuMig: a new human member of the chemokine family of cytokines. Biochem Biophys Res Commun 1993;192:223–30.
9. Arenberg DA, Kunkel SL, Polverini PJ, et al. Interferon-gamma-inducible protein 10 (IP-10) is an angiostatic factor that inhibits human non-small cell lung cancer (NSCLC) tumorigenesis and spontaneous metastases. J Exp Med 1996;184:981–92.
10. Hensbergen PJ, Wijnands PG, Schreurs MW, et al. The CXCR3 targeting chemokine CXCL11 has potent antitumor activity *in vivo* involving attraction of $CD8^+$ T lymphocytes but not inhibition of angiogenesis. J Immunother 2005;28:343–51.
11. Baltus T, von Hundelshausen P, Mause SF, et al. Differential and additive effects of platelet-derived chemokines on monocyte arrest on inflamed endothelium under flow conditions. J Leukoc Biol 2005;78:435–41.
12. Kasper B, Brandt E, Ernst M, Petersen F. Neutrophil adhesion to endothelial cells induced by platelet factor 4 requires sequential activation of Ras, Syk, and JNK MAP kinases. Blood 2006;107:1768–75.
13. Luster AD, Greenberg SM, Leder P. The IP-10 chemokine binds to a specific cell surface heparan sulfate site shared with platelet factor 4 and inhibits endothelial cell proliferation. J Exp Med 1995;182:219–31.
14. Petersen F, Bock L, Flad HD, Brandt E. A chondroitin sulfate proteoglycan on human neutrophils specifically binds platelet factor 4 and is involved in cell activation. J Immunol 1998;161:4347–55.
15. Lasagni L, Francalanci M, Annunziato F, et al. An alternatively spliced variant of CXCR3 mediates the inhibition of endothelial cell growth induced by IP-10, Mig, and I-TAC, and acts as functional receptor for platelet factor 4. J Exp Med 2003;197:1537–49.
16. Maione TE, Gray GS, Petro J, et al. Inhibition of angiogenesis by recombinant human platelet factor-4 and related peptides. Science 1990;247:77–9.
17. Sharpe RJ, Byers HR, Scott CF, Bauer SI, Maione TE. Growth inhibition of murine melanoma and human colon carcinoma by recombinant human platelet factor 4. J Natl Cancer Inst 1990;82:848–53.
18. Slungaard A. Platelet factor 4: a chemokine enigma. Int J Biochem Cell Biol 2005;37:1162–67.
19. Dana B, Carvalho AC, Ellman L. Plasma heparin neutralizing activity. Its use in the evaluation of thrombocytopenia and thrombocytosis. Am J Clin Pathol 1976;65:964–9.
20. Eslin DE, Zhang C, Samuels KJ, et al. Transgenic mice studies demonstrate a role for platelet factor 4 in thrombosis: dissociation between anticoagulant and antithrombotic effect of heparin. Blood 2004;104:3173–80.
21. Weber C. Platelets and chemokines in atherosclerosis: partners in crime. Circ Res 2005;96:612–6.
22. Gewirtz AM, Zhang J, Ratajczak J, et al. Chemokine regulation of human megakaryocytopoiesis. Blood 1995;86:2559–67.
23. Struyf S, Burdick MD, Proost P, Van Damme J, Strieter RM. Platelets release CXCL4L1, a nonallelic variant of the chemokine platelet factor-4/CXCL4 and potent inhibitor of angiogenesis. Circ Res 2004;95:855–7.
24. Addison CL, Belperio JA, Burdick MD, Strieter RM. Overexpression of the duffy antigen receptor for chemokines (DARC) by NSCLC tumor cells results in increased tumor necrosis. BMC Cancer 2004;4:28.
25. Sharma S, Yang SC, Hillinger S, et al. SLC/CCL21-mediated anti-tumor responses require IFNgamma, MIG/CXCL9 and IP-10/CXCL10. Mol Cancer 2003;2:22.
26. Van Coillie E, Van Aelst I, Wuyts A, et al. Tumor angiogenesis induced by granulocyte chemotactic protein-2 as a countercurrent principle. Am J Pathol 2001;159:1405–14.
27. Van Damme J, Proost P, Lenaerts J-P, Opdenakker G. Structural and functional identification of two human, tumor-derived monocyte chemotactic proteins (MCP-2 and MCP-3) belonging to the chemokine family. J Exp Med 1992;176:59–65.
28. Addison CL, Daniel TO, Burdick MD, et al. The CXC chemokine receptor 2, CXCR2, is the putative receptor for ELR^+ CXC chemokine-induced angiogenic activity. J Immunol 2000;165:5269–77.
29. Burdick MD, Murray LA, Keane MP, et al. CXCL11 attenuates bleomycin-induced pulmonary fibrosis via inhibition of vascular remodeling. Am J Respir Crit Care Med 2005;171:261–8.
30. Maione TE, Gray GS, Hunt AJ, Sharpe RJ. Inhibition of tumor growth in mice by an analogue of platelet factor 4 that lacks affinity for heparin and retains potent angiostatic activity. Cancer Res 1991;51:2077–83.
31. Arenberg DA, White ES, Burdick MD, Strom SR, Strieter RM. Improved survival in tumor-bearing SCID mice treated with interferon-gamma-inducible protein 10 (IP-10/CXCL10). Cancer Immunol Immunother 2001;50:533–8.
32. Addison CL, Arenberg DA, Morris SB, et al. The CXC chemokine, monokine induced by interferon-gamma, inhibits non-small cell lung carcinoma tumor growth and metastasis. Hum Gene Ther 2000;11:247–61.
33. Strieter RM, Burdick MD, Gomperts BN, Belperio JA,

Keane MP. CXC chemokines in angiogenesis. Cytokine Growth Factor Rev 2005;16:593–609.
34. Mantovani A, Allavena P, Sozzani S, et al. Chemokines in the recruitment and shaping of the leukocyte infiltrate of tumors. Semin Cancer Biol 2004;14:155–60.
35. Conti I, Rollins BJ. CCL2 (monocyte chemoattractant protein-1) and cancer. Semin Cancer Biol 2004;14:149–54.
36. Bikfalvi A, Gimenez-Gallego G. The control of angiogenesis and tumor invasion by platelet factor-4 and platelet factor-4-derived molecules. Semin Thromb Hemost 2004;30:137–44.
37. Yang J, Richmond A. The angiostatic activity of interferon-inducible protein-10/CXCL10 in human melanoma depends on binding to CXCR3 but not to glycosaminoglycan. Mol Ther 2004;9:846–55.
38. Soejima K, Rollins BJ. A functional IFN-gamma-inducible protein-10/CXCL10-specific receptor expressed by epithelial and endothelial cells that is neither CXCR3 nor glycosaminoglycan. J Immunol 2001;167:6576–82.
39. Murphy PM, Baggiolini M, Charo IF, et al. International union of pharmacology. XXII. Nomenclature for chemokine receptors. Pharmacol Rev 2000;52:145–76.
40. Hagedorn M, Zilberberg L, Wilting J, et al. Domain swapping in a COOH-terminal fragment of platelet factor 4 generates potent angiogenesis inhibitors. Cancer Res 2002;62:6884–90.
41. Nesmelova IV, Sham Y, Dudek AZ, et al. Platelet factor 4 and interleukin-8 CXC chemokine heterodimer formation modulates function at the quaternary structural level. J Biol Chem 2005;280:4948–58.
42. Perollet C, Han ZC, Savona C, Caen JP, Bikfalvi A. Platelet factor 4 modulates fibroblast growth factor 2 (FGF-2) activity and inhibits FGF-2 dimerization. Blood 1998;91:3289–99.
43. Opdenakker G, Van Damme J. The countercurrent principle in invasion and metastasis of cancer cells. Recent insights on the roles of chemokines. Int J Dev Biol 2004;48:519–27.
44. Müller A, Homey B, Soto H, et al. Involvement of chemokine receptors in breast cancer metastasis. Nature 2001;410:50–6.
45. Wetzel K, Struyf S, Van Damme J, et al. MCP-3 (CCL7) delivered by parvovirus MVMp reduces tumorigenicity of mouse melanoma cells through activation of T lymphocytes and NK cells. Int J Cancer 2007;120:1364–71.
46. Pan J, Burdick MD, Belperio JA, et al. CXCR3/CXCR3 ligand biological axis impairs RENCA tumor growth by a mechanism of immunoangiostasis. J Immunol 2006;176:1456–64.
47. Narvaiza I, Mazzolini G, Barajas M, et al. Intratumoral coinjection of two adenoviruses, one encoding the chemokine IFN-gamma-inducible protein-10 and another encoding IL-12, results in marked antitumoral synergy. J Immunol 2000;164:3112–22.